

Magnetic field dependence of sputtering magnetron efficiency

J. Goree and T. E. Sheridan

Department of Physics and Astronomy, The University of Iowa, Iowa City, Iowa 52242

(Received 4 September 1990; accepted for publication 31 May 1991)

A Monte Carlo simulation of electron transport is used to predict the dependence of the ionization efficiency on the magnetic field strength of a planar magnetron. This offers insight into the operation of the magnetron, and it also provides two valuable practical results.

First, the efficiency increases with field strength only up to a saturation level. Operating a magnetron with a stronger field strength would only lead to an undesirable loss of target utilization. Second, a scaling law is found that is useful for designing magnetrons of different sizes.

The magnetic field of a magnetron allows the operation of an intense sputtering discharge at low neutral gas densities.^{1,2} The magnetic field strength is a critical parameter in a magnetron design, but it is one that is often chosen in practice by empirical methods and guesswork. What is needed is a model that provides not only insight into magnetron operation, but also practical criteria for designing a magnetron.

Wendt *et al.*³ used a Hamiltonian model to predict that the etch track becomes wider and the sputtering target utilization improves as the field is made weaker, and they confirmed this prediction experimentally. This does not mean, though, that a weaker field is always better. There is trade-off. A weak field provides a wide etch track and good target utilization, while a strong field provides more effective electron confinement. In this letter we analyze the electron confinement as a function of magnetic field strength using Monte Carlo simulation. Based on our results, we offer practical criteria for designing planar magnetrons.

The device simulated here is the cylindrically symmetric planar magnetron⁴⁻⁸ shown in Fig. 1. The magnetic field B is formed by a cylindrical magnet and a concentric ring of 30 bar magnets, sandwiched between a nonferrous cathode and a steel pole piece. Because B is highly inhomogeneous, we specify that the field is measured at the point where it is tangential to the cathode target surface. The radius there is denoted as a , and the field magnitude as B_{tan} . In most devices, the etch track is deepest at radius a . For our device, $a = 1.7$ cm.

We have performed our simulations for various magnetic field strengths by adjusting B_{tan} in the code. This is equivalent to adjusting the magnetization M of the magnets. For comparison, Alnico 5 magnets yield $B_{tan} = 245$ G in the device shown in Fig. 1, as measured experimentally. The magnetic field shown in Fig. 1 was computed from the magnetic configuration.⁵ Although this field could be adapted to include the effect of the electronic $E \times B$ drift current parallel to the cathode, here we have not done so. The magnetic field due to this effect is at least an order of magnitude weaker than the field produced by the permanent magnets. For this letter, the shape of the field lines remains constant, regardless of the value selected for B_{tan} .

Of course one could also investigate other magnetic shapes using our method. The shape investigated here is a "type II unbalanced magnetron" in the notation of Window and Savvides.⁹ This means that the far-field dipole moment of the magnet assembly is dominated by the outer magnet ring. Our simulations⁴ and Langmuir probe measurements¹⁰ show that electrons escape from the plasma up the "chimney" along the center axis of this device. In contrast, our earlier simulations¹¹ have shown that electrons escape radially outward in the "type I" magnetron of Wendt *et al.*³

The electron Monte Carlo code, described in detail previously,^{4,8,11} ran as follows. An electron starts at rest from the cathode. Its orbit is computed by integrating the equation of motion with a fixed time step of 12 ps, which is much smaller than the mean time between collisions. The equation of motion includes the computed magnetic field and a prescribed, time-independent electric field.¹² The electric field is one dimensional, and it depends on the potential drop between the cathode and the plasma. We approximate that this drop is equal to the cathode bias

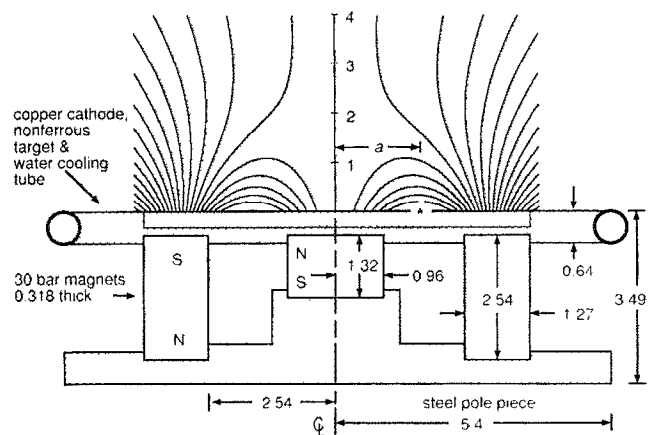


FIG. 1. Planar magnetron device. A cylindrical magnet is surrounded by a ring of 30 bar magnets, forming the field shown here. The magnetic field strength is characterized by its value B_{tan} at the radius a where it is tangential to the surface, as indicated by *. In the simulation, the magnetization M of the magnets and hence the value of B_{tan} can be adjusted without affecting the shape of the field. All dimensions are shown in cm.

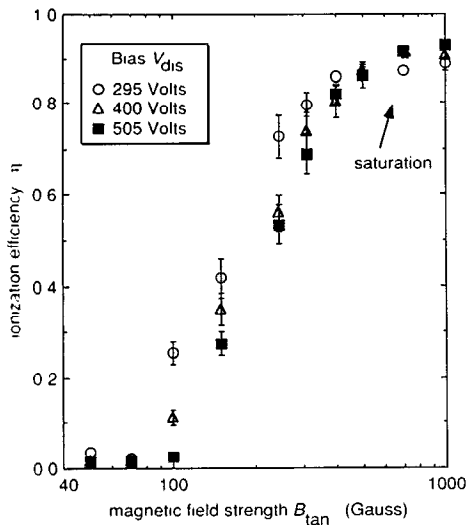


FIG. 2. Dependence of ionization efficiency, defined by Eq. (1), on the magnetic field strength B_{tan} . The ionization efficiency increases with magnetic field strength only up to saturation at $\eta = 0.9$. The simulation assumed a neutral argon density corresponding to a pressure of 2 Pa at room temperature. They were repeated for the cathode biases; $V_{\text{dis}} = 295, 400,$ and 505 V, which correspond to $N_{\text{max}} = 13, 17$ and 21 . One-standard-deviation error bars are shown.

V_{dis} because the plasma potential is small in comparison. Elastic, excitation, and ionizing collisions with neutrals occur at random intervals,⁴ and they reduce the electron's energy and scatter its velocity direction.⁸ The particle's orbit is terminated when its total energy drops below the ionization potential, or when it escapes the region where the field lines are drawn in Fig. 1. The next electron is then started on the cathode at a radius chosen randomly in the self-consistent manner described in Ref. 4. This procedure was repeated for an ensemble of 30–200 electrons.

For this letter we used the simulation to find the ionization efficiency by cathode emission η , which has been defined as follows.⁸ The number of ionizations that a single electron performs, averaged over an ensemble of electrons, is denoted by $\langle N_i \rangle$. We can compare $\langle N_i \rangle$ to the maximum possible number of ionization $N_{i\text{max}}$ that can be performed by a well-confined electron in the absence of excitation collisions.⁸ The ionization efficiency is the ratio

$$\eta \equiv \langle N_i \rangle / N_{i\text{max}}, \quad (1)$$

and it will depend on the magnetic field, pressure, and cathode bias. The efficiency η lies between zero and an upper limit^{4,8} of about 0.9.

We allow ionization only by electrons born on the cathode, and ignore ionization by electrons born in the sheath and in the main plasma. Earlier simulations⁹ showed that this approximation causes the simulation to underestimate η somewhat for a magnetron with a weak field of $B_{\text{tan}} = 104$ G.

Results for the ionization efficiency at various field strengths and cathode biases are presented in Fig. 2, which shows that η increases with magnetic field strength only up to a saturation level, $\eta = 0.9$. The simulation was run for argon at only one density (corresponding to 2 Pa at room

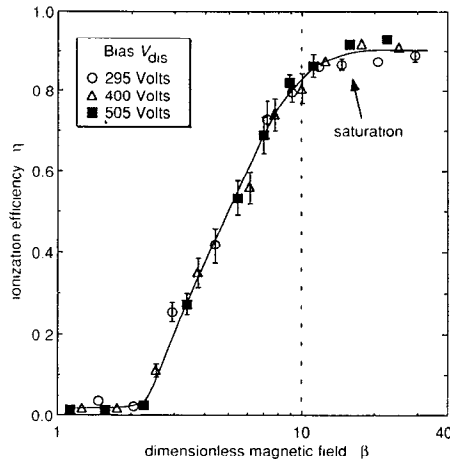


FIG. 3. Dependence of ionization efficiency η on the dimensionless parameter $\beta = 0.2965 B_{\text{tan}} a / V_{\text{dis}}^{1/2}$, where B_{tan} is in G, a in cm, and V_{dis} in V. The simulation results lie on a similarity curve that saturates at $\beta \approx 12-15$. Using a magnetic field stronger than required for the onset of saturation will not yield any increase in ionization efficiency.

temperature) because we have found⁸ that the neutral density has only a weak effect on η .

It is useful to seek a law of similarity that makes all the curves in Fig. 2 coincide. This is accomplished by constructing a dimensionless variable from the parameters B_{tan} , V_{dis} , and a :

$$\beta \equiv \sqrt{e/2m} (a/V_{\text{dis}}^{1/2}) B_{\text{tan}}. \quad (2)$$

Here e and m are the electron charge and mass. Equation (2) is $\beta = 0.2965 B_{\text{tan}} a / V_{\text{dis}}^{1/2}$ in practical units (G, cm, and V). Figure 3 confirms that the efficiency η is a function of β and that the data lie on a similarity curve. The efficiency increases with β until it saturates for $\beta \geq 15$. This similarity curve and the scaling law in Eq. (2) are the principal results of this letter.

Using a magnetic field stronger than the saturation level in Fig. 3 offers no benefit. Indeed, it would result in an undesirable loss of etch track width and target utilization. The model of Wendt *et al.*³ predicts that the etch track width is proportional to $a\beta^{-1/2}$. This scaling implies that the target utilization is $\propto \beta^{-1/2}$, and is thus improved by using a weaker magnetic field.

For completeness, we outline here a derivation of Eq. 2. The portion of Fig. 2 where the curves do not coincide is the transitional regime below saturation, which arises from electrons that are scattered into unconfined orbits and are lost before they consume their energy by ionizations.⁸ In a Hamiltonian formalism, orbits can be predicted by the effective potential energy surface Ψ .^{3,4} Unconfined orbits are lost through a hole in the surface, as shown in Fig. 3 of Ref. 4. Using a cylindrical coordinate system (r, θ, z) and conservation of canonical angular momentum,⁴ we find that for an electron born at rest on the cathode at radius r_0 :

$$\Psi(r, z) = e^2 [r_0 A_{\theta 0} - r A_{\theta}(r, z)]^2 / 2mr^2 - e\phi(z), \quad (3)$$

which has units of energy. The first term of Eq. (3) is due to the magnetic field, and it prevents electrons from mov-

ing a large distance from the cathode. Here A_θ is the azimuthal component of the vector potential, defined by $\mathbf{B} = \nabla \times \mathbf{A}$. The value of A_θ at the electron's birthplace is denoted $A_{\theta 0}$. The second term is due to the electric potential ϕ , which repels electrons from the cathode.

Now consider scaling the system: one may vary the electric potential, the magnetization, and the magnetron size. These quantities are parameterized by V_{dis} , M , and a , respectively. (The gas pressure can also be altered by gas rarefaction effect or by the user, but the effect is negligible because the ionization efficiency is almost independent of gas density.⁸) The field strength B_{tan} is proportional to M . In varying the size, the dimensions of the magnets and the gaps between them retain the same proportions. The vector potentials A_θ and $A_{\theta 0}$ scale as aM , while r and r_0 scale as a , so that the first term of Eq. (3) scales as $(aM)^2$. The electric potential ϕ in the second term scales as V_{dis} . Likewise, an electron born on the cathode has an energy that scales as V_{dis} . If a , M , and V_{dis} are increased while holding the ratio $(aM)^2/V_{\text{dis}}$ constant, then the potential surface shape Ψ/V_{dis} will not change. The proportions of a hole in the surface will be unaffected by the scaling, so that an electron born on the cathode will still be lost after the same number of bounces. Provided that the mean-free path is $\geq a$, the electron will perform no more ionizations after it escapes through the hole.^{4,8} The ionization efficiency thus will be unchanged by the scaling. This scaling, the ratio of the two terms in Eq. (3), yields the dimensionless variable β in Eq. (2).

As noted earlier, there is a design trade-off in increasing the field strength. If the field is weaker than required for saturation, one sacrifices target utilization for ionization efficiency. Beyond the saturation level, however, there is no longer a trade-off in using a field stronger than required for saturation—things only get worse with increasing field strength. In particular, the target utilization suffers without improving the ionization efficiency. This result of our model is of practical use. It is contrary to a conventional wisdom that a stronger field is always better.

Let us now assess the range of parameters where the simulation is valid. A wide variety of experimental data, including Langmuir probe, laser-induced fluorescence, optical glow, and etch track profile measurements,^{4,7,8,11} have proven the accuracy of the model for two sets of parameters: $B_{\text{tan}} = 245$ G, $a = 1.7$ cm, $\beta = 7$, and $B_{\text{tan}} = 277$ G, $a = 5$ cm, and $\beta = 22$. So the simulation appears to be accurate in that range of parameters. Where is it not accurate? It was found¹¹ to predict too low a value for η for a weak field of $B_{\text{tan}} = 104$ G (due to a violation of the assumption that electrons emitted from the cathode dominate the ionization). We also suspect that the prescribed electric field model will fail at saturated field strengths of $\beta > 20$, if the plasma potential becomes very negative. Based

on these limits, we can say that the onset of saturation (our principal result) is probably predicted with enough accuracy, provided that $B_{\text{tan}} \geq 104$ G.

We summarize with two criteria for magnetron design. First, for designs of different sizes but the same proportions, a larger magnetron should have magnets with a weaker magnetization. This will provide a weaker B_{tan} in order to keep β equal to a constant in Eq. (2). (This law is valid provided that the magnetron radius a is not much larger than the mean free path.) Second, for maximum efficiency of ionization by electrons emitted from the cathode, the magnetic field strength should be selected to operate at the onset of saturation in Fig. 3. This occurs at $\beta \approx 12$ – 15 for a cylindrically symmetric planar magnetron with the proportions shown in Fig. 1. It would be undesirable to use a stronger field because it would decrease the target utilization without increasing the ionization efficiency.

As a sputtering target is consumed, its surface becomes closer to the magnets so that the magnetic field there grows in time. A magnetron designer might wish to maximize the sputtering rate averaged over the target lifetime. In that case, the magnetron should be designed to start at a weaker field, perhaps $\beta \approx 8$ – 10 , when a fresh target is in place. The corresponding field strength in Gauss can be determined from Eq. (2). For a magnetron of radius $a = 1.7$ cm operated at $V_{\text{dis}} = 400$ V, the optimal field strength for a fresh target would be $B_{\text{tan}} \approx 310$ – 395 G.

This work was supported by the Iowa Department of Economic Development.

¹John A. Thornton and Alan S. Penfold, "Cylindrical magnetron sputtering," in *Thin Film Processes*, edited by J. L. Vossen and W. Kern (Academic, New York, 1978), p. 75.

²Robert K. Waits, in *Thin Film Processes*, edited by J. L. Vossen and W. Kern (Academic, New York, 1978), p. 131.

³A. E. Wendt, M. A. Lieberman, and H. Meuth, *J. Vac. Sci. Technol. A* **6** 1827 (1988). The experiment therein was characterized by $7 < \beta < 25$.

⁴T. E. Sheridan, M. J. Goeckner, and J. Goree, *J. Vac. Sci. Technol. A* **8**, 30 (1990).

⁵T. E. Sheridan and J. Goree, *J. Vac. Sci. Technol. A* **7**, 1014 (1989), reported the magnetic field computed in two dimensions from a magnetic scalar formalism. The effect of the pole piece was modeled by using image magnets, and the 30 individual bar magnets in the outer ring were treated as a solid annulus with a reduced magnetization to account for the gaps between bars. This field was confirmed against experimental data.

⁶T. E. Sheridan, M. J. Goeckner, and J. Goree, *J. Vac. Sci. Technol. A* **8**, 1623 (1990).

⁷M. J. Goeckner, J. Goree, and T. E. Sheridan, *IEEE Trans. Plasma Sci.* **19**, 301 (1991).

⁸T. E. Sheridan, M. J. Goeckner, and J. Goree, *Appl. Phys. Lett.* **57**, 2080 (1990).

⁹B. Window and N. Savvides, *J. Vac. Sci. Technol. A* **4**, 196 (1986).

¹⁰T. E. Sheridan, M. J. Goeckner, and J. Goree, *J. Vac. Sci. Technol. A* **9**, 688 (1991).

¹¹J. E. Miranda, M. J. Goeckner, J. Goree, and T. E. Sheridan, *J. Vac. Sci. Technol. A* **8**, 1627 (1990).

¹²T. E. Sheridan and J. Goree, *IEEE Trans. Plasma Sci.* **17**, 884 (1989).